A Lens Collar Auto-inspection System

Chien-Chih Wang
Department of Industrial Engineering and Management, Ming Chi University of Technology
84 Gungjuan Rd., Taishan Dist., New Taipei City 24301, Taiwan, Republic of China
Email: ieccwang@mail.mcut.edu.tw

Ssu-Han Chen*
Department of Industrial Engineering and Management, Ming Chi University of Technology
84 Gungjuan Rd., Taishan Dist., New Taipei City 24301, Taiwan, Republic of China
*Corresponding author email: ssuhanchen@mail.mcut.edu.tw

Abstract

Surface quality of lens collar arouses customers' highly concern. Manual inspection has been a way for quality assurance, but it might cause employees injuries and strenuosity. So it is worthy to introduce a nondestructive inspection system. The proposed system is composed of a CCD, a white LED coaxial light and a motor. The region of interesting (ROI) of lens collar is extracted firstly where is filled with statistical texture. The discrete cosine transformation (DCT) image restoration sub-function reflects textures into high energy components which are then be oppressed by filters. We finally attempt to highlight the defects by defect detection sub-function because of gray levels of textures within a range of limit while defects not.

1. Introduction

Single-lens cameras have increasingly expanded its market to common consumers with lower price. Taiwan has focused its expansion on this camera market and launched new blueprint for next camera original equipment manufacturer industries. One of components in the lens of single-lens camera is lens collar which is used to fix lens and connects aperture or adjustable ring. The lens is cut by the diamond cutter in wash bed with CNC, then it is finished by electroplating on its surface. Unfortunately, the manufacturing process of lens is always going badly with the problems of over high reject ratio. The customers have quite a strictly demands on lens' appearance when receive it, admitting of no overfull blemishes, therefore, manufacturers are required to assure the quality on lens collar surface. Inspector is asked to give a fully manual check to each lens collar so as to ensure the quality before handing in. Manual inspection is time-consuming and strenuous, thus, the study intends to design the system that is capable of auto-detecting defects on lens collar with the help of machine vision.

As lens collar featured cambered metal material, the study mainly face the characteristics of the detection on highly specular reflection (HSR) and non-plated surface. The gleaming metal surface usually reflects light that happens in area to-be-inspected made most sensors break to affect image's quality easily. Others, non-plated will make light intensity scattered in bed or band shape. Therefore, the hardware should plan to remove the problems of reflection and uneven light, as well as to highlight defects appropriately. The study inspired by papers overview [1-4] puts on several leading knowledge on hardware design. First of all, the normal vector angle of CCD and checked surface is advised to design to orthogonal to make surface of tested things lighting equably. Second, ring-type, ball-type and on-axis light all possess of reflective ability. Finally, capture a little board of image every time can reduce cambered effect to increase the resolution.

Another breakthrough of the study is for the first time the implication of image restoration scheme based on DCT on interspersed statistical textures to defect detection, which is help to find out the defects embedded in textures, to avoid the feature elected problem of feature extraction methods and to get rid of calibration process of template matching method. From the previous researches, we know that discrete Fourier transformation (DFT) and discrete wavelet transformation (DWT) have been tested to simultaneously apply in regular and statistic texture defects [4-9], while DCT only in regular texture defect detection [10]. Due to the rare of applied studies for statistic texture defect detection, the study's DCT experiment is also one of the contributions.

2. Research Methods

The study takes the most wild used lens collar with 48mm outside diameter as the inspected objective, whose side view is as what Figure 1 show. The red region represents the region of interesting (ROI). We especially put plastic sheeting in inner ring to make the viewer learn usage of lens collar more clearly.

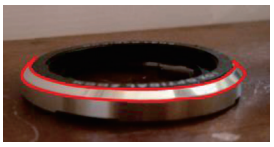

Figure 1. The side view of lens collar.

2.1 Hardware Structure

Refer to Figure 2, the proposed system consists of image-captured module, light resource and motor. The work piece was put above motor after hold by a ring-shaped fixer. The normal vector of CCD and optical axis of lens collar is to be orthogonal. White LED coaxial ring light source is installed between lens collar and CCD. To expose the defects, the study is avoided of direct light radiates it because the work piece surface features high reflection so that the incident light will generate reflected light depended on incident angle to come into being dark-field illumination. In turn, the un

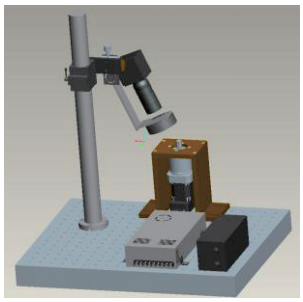

Figure 2. The configuration of lens collar auto-inspection system.

even defect will change light path to allow partial reflected light into CCD, and to form black based textures. As Figure 3 shows, collar is represented by statistic textures, on which there is scratch, jelly, punctiform, uneven electroplating or other defects.

2.2 Defect Detection Algorithm

For inspecting defects automatically, this study proposed an algorithm, covering image segmentation, DCT-based image restoration scheme and defect detection, which will be respectively described in following, and the flow chart is introduced in Figure 3.

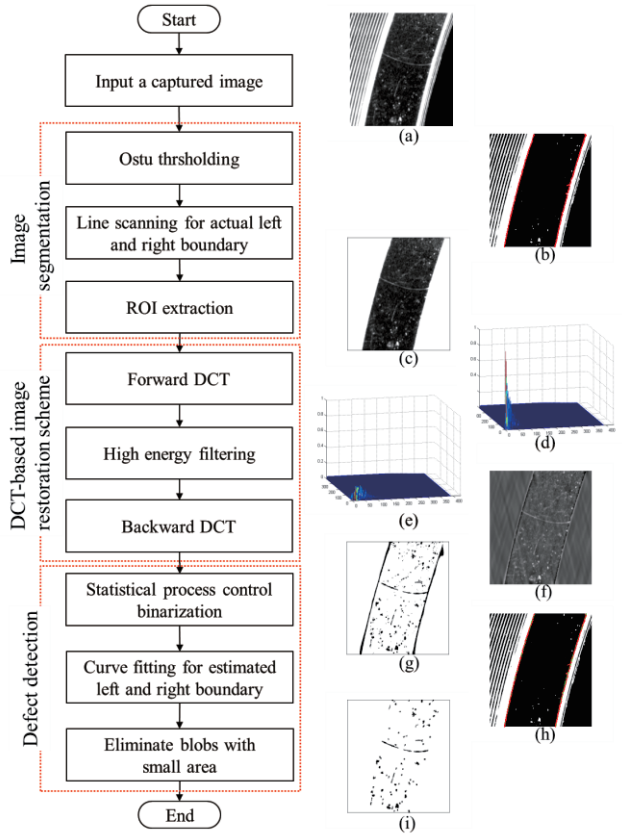

Figure 3: Flowchart of proposed defect detection algorithm. (a) the captured image of lens collar; (b) actual boundary; (c) image after image segmentation; (d) specturm image; (e) north-rejected filters on the specturm; (f) restored image; (g) image after statistical process control binarization; (h) actual and estimated left and right boundary; (i) image after curve fitting and blob analysis.

(1) Image Segmentation: To reduce the interference of subsequent image processing, we extract the ROI only, whose principle is to locate collar by the chamfered and polished plane of the left and right collar. This study takes the blob whose area is larger than area median and angle is equal to angle mode (accurate to ten digits) as the candidate chamfered and polished plane, in which the former is the one with top two area and smaller y axis, while the latter with bigger y axis as shown in red curve of Figure 3(b). Then Figure 3(a) is segmented based on the coordination of red curves and the outcome is as what Figure 3(c) shows.

(2) DCT-based Image Restoration Scheme: To detect defects in lens collar image filled with statistic texture, this study uses DCT-based image restoration scheme to blur texture, which is a breakthrough as this it is rare to apply the method to defect detection of statistic texture, yet it is often to apply it to defect of regular texture [10]. After getting the lens collar image of a vision showed Figure 3(c), DCT will transfer the image into frequency domain C(u, v) by

$$C(u,v) = \alpha(u)\times\alpha(v)\sum_{x=0}^{m-1}\sum_{y=0}^{n-1} f(x,y)\times \cos\left[\frac{(2x+1)u\pi}{2m}\right]\times\cos\left[\frac{(2y+1)v\pi}{2n}\right] \quad (1)$$

, where f(x, y) means gray value of pixel coordinate, u = 0, 1, 2, ..., m–1, v = 0, 1, 2, ... , n–1, while α(u) and α(v) defined as

$$\alpha(u) = \begin{cases} \sqrt{\frac{1}{m}}, & u = 0 \\ \sqrt{\frac{2}{m}}, & u = 1,2,\ \ldots, m-1 \end{cases}$$
$$\alpha(v) = \begin{cases} \sqrt{\frac{1}{n}}, & v = 0 \\ \sqrt{\frac{2}{n}}, & v = 1,2,\ \ldots, n-1 \end{cases} \quad (2)$$

Next is to map F(u, v) with enlarged dynamic range to P(u, v) with 0-1 value in

$$P(u,v) = S\left[\log\left(1+|C(u,v)|^2\right)\right] \quad (3)$$

Thereinto, S(•) is scaling operator. Look Figure 3(d), lens collar has transferred into frequency domain. If one intends to blur statistic textures in spatial domain, one can eliminate high energy components represented textures by notch-rejected filters in Equation 4 at frequency domain. High energy components represented textures will center around frequency domain as shown in Figure 3(e).

$$C(u,v) = \begin{cases} 0 & , \text{if } P(u,v) \geq k1 \\ C(u,v) & , \text{o.w.} \end{cases} \quad (4)$$

k1∈[0, 1] means high-energy threshold that targets to get rid of textures and to preserve defects.

Next, backward DCT of Figure 3(f) in Equation 5 makes image in frequency domain reverse to spatial domain as Figure 6(c) shows; the result is called restored image.

$$\hat{f}(x,y) = \sum_{u=0}^{m-1}\sum_{v=0}^{n-1} \alpha(u)\times\alpha(v)\times C(u,v)\times \cos\left[\frac{(2x+1)u\pi}{2m}\right]\times\cos\left[\frac{(2y+1)v\pi}{2n}\right] \quad (5)$$

Among, $x = 0, 1, 2, ..., m–1$, $y = 0, 1, 2, ... , n–1$. Observing Figure 3(f), we find that statistic textures of restored image has been blurred, whose gray value has been limited within even range; in turn, gray value of defects has been kept and more brighter.

(3) Defect Detection: To show defects in restored image, three procedures are designed. Firstly, as shown in Figure 3(f), it is available to set up upper control limit (UCL) by Equation 6 statistical process control binarization method to expose relatively brighter defects because texture pixel of restored image has become even and limited within a certain range.

$$\hat{f}(x,y) = \begin{cases} 1, \text{ if } \hat{f}(x,y) < \mu_{\hat{f}} + k2\cdot\sigma_{\hat{f}} \\ 0, \text{ o.w.} \end{cases} \quad (6)$$

Among, k2 is control constant, $\mu_{\hat{f}}$ and $\sigma_{\hat{f}}$ respectively are average and standard deviation of restored image gray value. Figure 3(g) shows if a pixel's gray value locates in UCL, it would be represented by white and means texture pixel that should be eliminated originally; if not, it would be represented by black and means the defect pixel that should be kept.

However, compared Figure 3(c) with Figure 3(g), we find that there are many false alarm on binarized image dealt by Equation 6, which is mainly happened outside lens collar boundary, in that DCT itself is able to detect and contrast violent change, so as to brighter lens collar boundary in restored image by Equation 6. To avoid of misjudging, this study is to find out relative smooth estimated left and right boundary by back-propagation neural network (BPNN), which is mainly to find out relative smooth estimated boundary through the curve its fitting ability. Curve fitting is a simple question here, so the study set network structure of BNPP as 1×1×1, there into the first 1, input number, is the x axis coordinate sequence of actual boundary, the second 1 is the neuron number of hidden layer, the third 1, output number, is the y axis coordinate sequence of actual boundary. The fitting results are shown as Figure 3(h); the red curve represents actual boundary, while green curve the estimated boundary. The estimated boundary represents one perfect collar boundary, whose feature is beneficial for the research to compare and find out twist and turn. Finally, it is necessary to eliminate blobs with smaller area, whose area threshold can be made as needs. The ultimate result is shown as Figure 3(i).

3. Experiment Results

In this section, except discussing parameter sensitive analysis of system, this study also tests the system's performance.

3.1 Parameters Sensitivity Experiment

It is needed to find out appropriate parameter setting value by training before actual operation on this system. The system has two parameter: highly energy threshold (k1) and control constant (k2). To get steady k1 and k2 values, this study operates defect detection algorithm with different combinations of k1 = 0.10, 0.11, …, 0.50 and k2 = 0.6, 0.7, …, 3.5, and records the corresponding detection average accuracy rate. As Figure 4 shows, k1 and k2 value between 0.49 and 0.53, and 2.3 and 2.7, the detection accuracy rate reaches its peak; while other parameters combinations may produce more false alarm or missed detection.

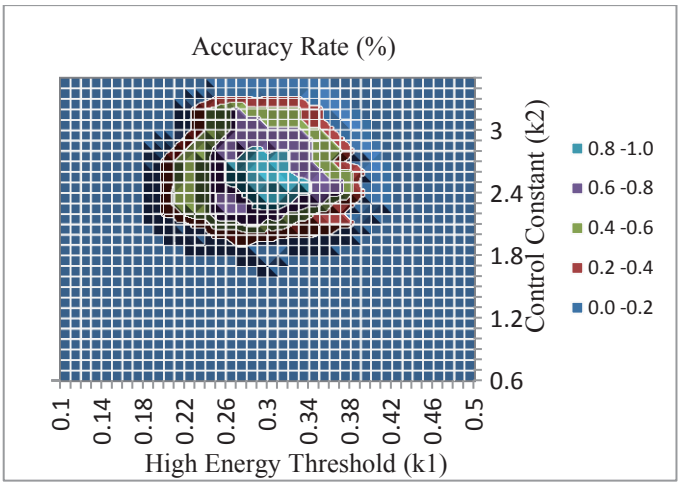

Figure 4: The sensitivity analysis of accuracy rate under different k1and k2.

3.2 Demonstrating of Inspection Results

To show system's test ability, the study verify it with several testing samples, among which parameters are set by median value of suggested area decided by previous sub-section, namely, k1 = 0.30, k2 = 2.5.Based on some lens collar image in Figures 5(a1)-5(a4), after operating detection algorithm, the research get the binarized image of Figures 5(b1)-5(b4). One image without defect would feedback one pure response diagram; otherwise, one response figure with rough defect shape and location are answered.

4. Conclusion

Defect detection of lens collar has traditionally depended on manual inspection that has low efficiency as intense light; even the well-trained inspectors cannot meet the quality standard needs. To increase detection steadily, this study puts on AOI system of lens collar surface, which is help to overcome inspector with non-plated and HSR characteristics. Non-plated circumstance gets lens collar surface image of different views sequentially to

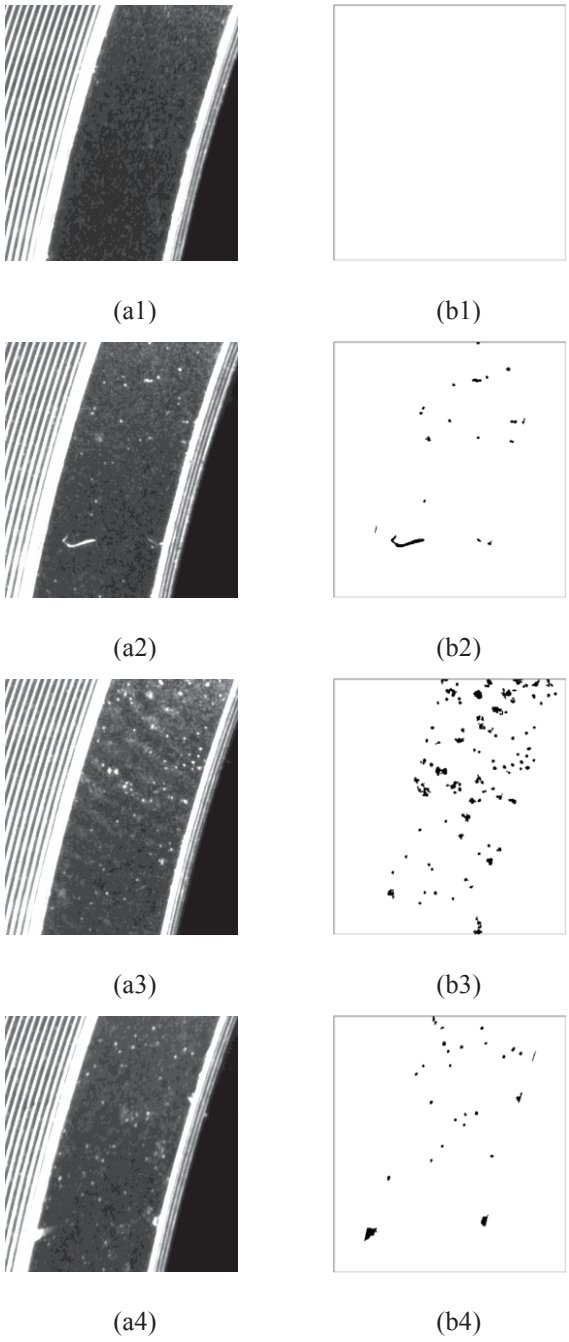

Figure 5: Experimental result. (a1) lens collar without defects; (a2) lens collar with scratch and punctiform; (a3) lens collar with punctiform and defects on edge; (a4) lens collar with punctiform and electroplating; (b1)-(b4) equivalent binarization image.

overcome, while HRS is designed as dark field illumination to avoid of normal collar surface's intense and bright collar's imaging. After capturing the image, ROI will be auto-segmented. Then the statistic textures on lens collar will be eliminated by DCT-based image restoration scheme and defects be kept. Finally, the defects will be showed by defect detection sub-function. The result shows that the system has better detection efficiency with a high accuracy rate to ensure lens collar quality.

Acknowledgments

This research is partially supported by the Ministry of Science and Technology, Taiwan, under contract no. NSC 102-2218-E-131-002- and MOST 103-2221-E-131-028-

References

[1] G. Rosati, et al.: "Real-time defect detection on highly reflective curved surfaces," *Optics and Lasers in Engineering*, vol.47, pp.379-384, 2009.

[2] X. W. Zhang, et al.: "A vision inspection system for the surface defects of strongly reflected metal based on multi-class SVM," Expert Systems with Applications, vol.38, pp.5930-5939, 2011.

[3] C. J. Li, et al.: "Developing a new automatic vision defect inspection system for curved surfaces with highly specular reflection," *International Journal of Innovative Computing, Information and Control*, vol.8, no.7B, pp.5121-5136, 2012.

[4] D. B. Perng, et al.: "A novel internal thread defect auto-inspection system," *International Journal of Advanced Manufacturing Technology*, vol.47, no.5-8, pp.731-743, 2010.

[5] D. M. Tsai, et al.: "Automated surface inspection for statistical textures," *Image and Vision Computing*, vol.21, no.4, pp.307-323, 2003.

[6] S. H. Chen, et al.: "Automatic optical inspection system for IC molding surface," *Journal of Intelligent Manufacturing*, 2014, DOI: 10.1007/s10845-014-0924-.

[7] D. M. Tsai, et al.: "Automatic band selection for wavelet reconstruction in the application of defect detection," *Image and Vision Computing*, vol.21, no.5, pp.413-431, 2003.

[8] T. S. Li,: "Applying wavelets transform and support vector machine for copper clad laminate defects classification," *Computers & Industrial Engineering*, vol.56, no.3, pp.1154-1168, 2009.

[9] W. K. Wong, et al.: "Stitching defect detection and classification using wavelet transform and BP neural network," *Expert Systems with Applications*, vol.36, no.2, pp.3845-3856, 2009.

[10] D. B. Perng, et al.: "Directional textures auto-inspection using discrete cosine transform," *International Journal of Production Research*, vol.49, no.23, pp.7171-7187.